Nonlinear dynamics of a laser diode with injection of an optical frequency comb

Yaya Doumbia, Tushar Malica, Delphine Wolfersberger, Krassimir Panajotov, Marc Sciamanna

Nonlinear dynamics of a laser diode with injection of an optical frequency comb

YAYA DOUMBIA,[1,2*] TUSHAR MALICA,[1,2] DELPHINE WOLFERSBERGER, [1,2] KRASSIMIR PANAJOTOV,[3,4] AND MARC SCIAMANNA [1,2]

[1] *Chaire Photonique, LMOPS, CentraleSupélec, 2 Rue Edouard Belin 57070 Metz, France*
[2] *Université de Lorraine, LMOPS, 2 Rue Edouard Belin 57070 Metz, France*
[3] *Brussels Photonics Group (B-PHOT), Vrije Universiteit Brussel, Brussels, Belgium*
[4] *Institute of Solid State Physics, Bulgarian Academy of Sciences, Sofia, Bulgaria*
[*] *yaya.doumbia@centralesupelec.fr*

Abstract: We experimentally and theoretically demonstrate the variety of the nonlinear dynamics exhibited by a single frequency semiconductor laser subjected to optical injection from a frequency comb. The injection parameters (the detuning and the injection strength) and the comb properties (comb spacing and the amplitude of the injected comb lines) are varied to unveil several dynamics such as injection locking, wave-mixing, chaotic dynamics, and unlocked time-periodic dynamics corresponding to new comb solutions. The asymmetry of the injected comb is shown to modify the size of the injection locking region in the parameter space, as well as the common properties between the new comb solutions observed and the injected comb.

1. Introduction

The entrainment of the intrinsic oscillation frequency of the laser using an external oscillator has been of interest in the past forty years [1–3]. When the detuning frequency $\Delta\nu$, i.e, the difference between the external oscillator frequency and the intrinsic oscillation frequency of the injected laser, is sufficiently small, the intrinsic oscillation frequency of the injected laser becomes entrained by the external oscillator leading to so-called injection locking [4, 5]. Often, outside the region of parameters leading to the injection locking, the laser bifurcates to more complex nonlinear dynamics including route to chaos [6–9], extreme events [10], intermittency [5] and mode switching such as in VCSELs [11, 12]. These nonlinear dynamics, in turn, open the path towards new applications in all-optical signal processing [13], microwave signal generation [14] and frequency comb generation [15].

More recently, optical injection dynamics of a laser diode when being injected, not by a single laser line, but by a frequency comb have been studied. Injection locking [16, 17] has been reported and characterised by selective amplification (SA) of the comb line that shows the smallest detuning from the injected laser frequency. A laser, injected with a frequency comb has been observed to exhibit a different solution of injection locking compared to the one in case of single frequency injection [18]. Some researchers have also analysed the variation in the amplitude of the comb lines when varying the injection parameters (detuning and injection strength) and the comb properties (comb spacing and number of injected comb lines) [19–21]. Of particular interest is the possibility to tune the relative amplitudes of the comb lines by optical injection. Recent works have further questioned the possibility of resonance between the comb spacing and the relaxation oscillation frequency [21–23]. In the field of theoretical research, simulations of rate equations have also predicted a rich variety of nonlinear dynamics [24]. The optical injection with a frequency comb has found applications in various fields such as demultiplexing of optical frequency comb [25, 26], optical frequency metrology [27] and optical communication [25]. The question of how the optical injection with a frequency comb interplays

with the injection induced nonlinear dynamics is however not fully addressed yet.

In this Letter we experimentally demonstrate the nonlinear dynamics of a single frequency laser under optical injection with a frequency comb. The injection locking solution documented in the literature [19, 21, 25] is identified here as selective amplification (SA) in which the injected laser selectively amplifies and locks to the injected with the smallest detuning. There are therefore as many SA solutions as the number of injected comb lines. In addition, we report new comb solutions observed to have some properties in common with the injected comb. We also control and optimize the generated comb properties with the injection parameters. One of the challenges in the field of combs is indeed the simultaneous control of the comb while maintaining a superior quality of comb flatness. Furthermore, to our knowledge, the dynamics of a single frequency laser subjected to a non-flat comb, i.e, an asymmetric comb injection closer to the real experimental configuration, has not been addressed yet. We analyze the impact of the asymmetry of the injected comb on the injected laser dynamics particularly on the dynamics of new comb solutions and on the injection locking solution. The results of this work are in good agreement with our recent theoretical predictions [24]. We also show new numerical simulations to analyse the impact of the asymmetry of the injected comb, the results of which are again in agreement with our experimental observations.

2. Experimental mapping of nonlinear dynamics

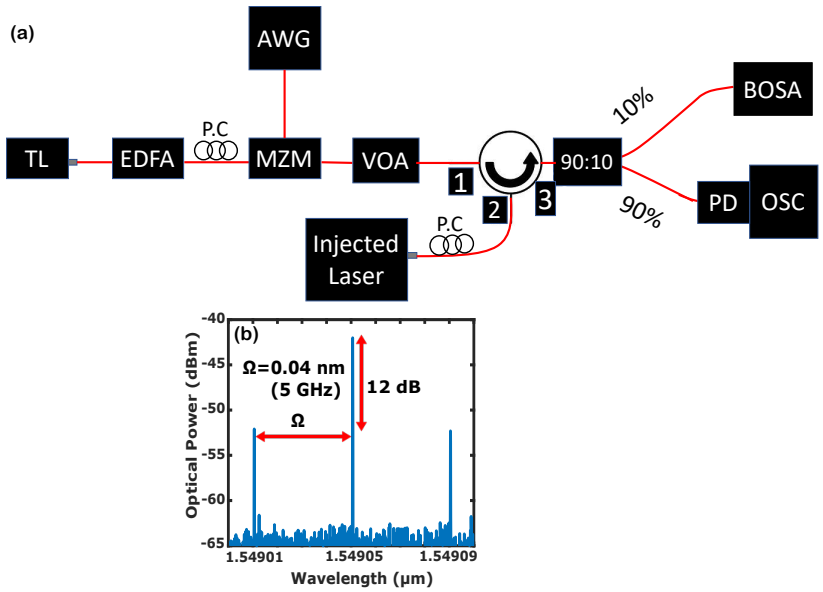

Fig. 1. (a) Experimental setup for frequency comb injection. TL: Tunable Laser, EDFA: amplifier, P.C: Polarization Controller, AWG: Arbitrary Waveform Generator, MZM: Mach-Zehnder Modulator, VOA: Variable Optical Attenuator, OSA: Optical Spectrum Analyser, PD: photodiode, OSC: Oscilloscope. (b) optical spectrum of the injected comb

Figure 1 (a) shows the experimental setup for the optical injection with a frequency comb. The output of a continuous-wave (CW) tunable laser (Yanista Tunics T100S) is first amplified by an Erbium-Doped Fiber Amplifier (EDFA). The linewidth of the tunable laser is around 30 MHz. An electric signal modulation is generated by an Arbitrary Waveform Generator (AWG) (Tektronix AWG 700002A) and sent to the RF port of a Mach-Zehnder (MZ) Modulator. The

first polarisation controller (P.C) is used to align the laser polarisation with the input of the MZ modulator. The MZ modulator is a $LiNbO_3$ with a 12.5 GHz bandwidth. Optical comb with 3 optical frequency lines is generated in the output of the MZ modulator. The comb's optical power is controlled using a variable optical attenuator (VOA). The injected laser is a Distributed feedback (DFB) laser emitting ~ 1549.7 nm with an approximate threshold current of 8 mA and maintained at 20° C. The fiber circulator is arranged to provide isolation for the injected laser. The injected laser dynamics is analyzed with a high resolution optical spectrum analyzer BOSA 400, which allows monitoring optical spectra with a resolution of about minimum 0.1 pm or 10 MHz at the operating wavelength of 1550 nm. The second polarization controller (P.C) allows controlling the polarization of the injected light. The temporal output is measured with a real-time digital oscilloscope (OSC) with sampling rate of 50 GSamples/s. A photodiode (PD) (Newport 1544-B) 12 GHz bandwidth is placed at the input of the oscilloscope to convert optical signal to an electrical signal. Figure 1 (b) shows the optical spectrum of the injected comb. This figure is obtained for a fixed comb spacing (Ω). The difference between the power of the central comb line and the sides comb lines is around 12 dB. In the following text, the frequency detuning is defined with respect to the frequency of the central comb line, i.e., $\Delta\nu = \nu - \nu_0$, where ν and ν_0 are the frequencies of the central injected comb line and the injected laser, respectively.

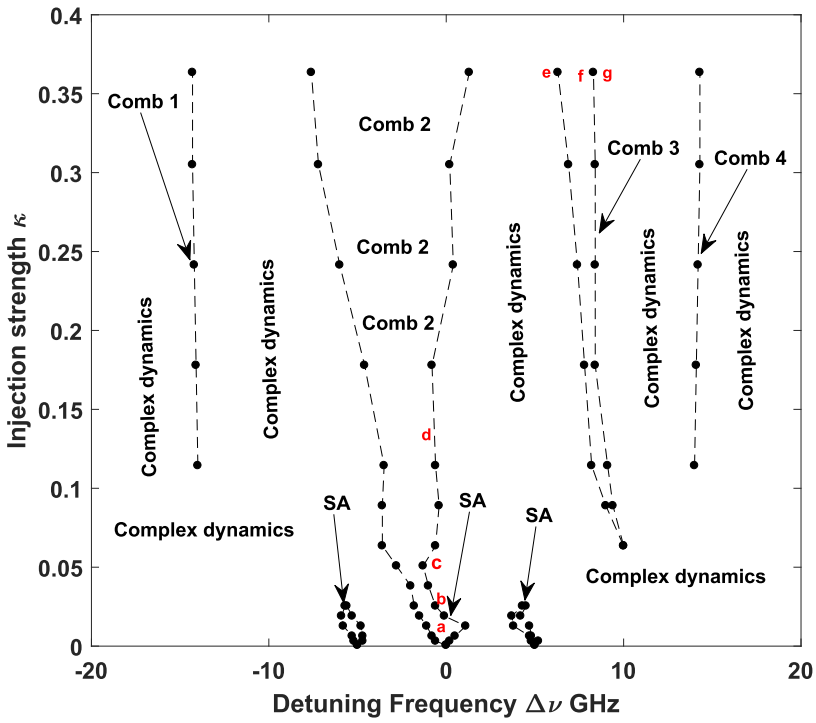

Fig. 2. Experimental dynamical mapping of single frequency laser subject to an optical injection from a frequency comb for Ω = 5 GHz. Several regions are observed: SA: Selective amplification, Unlocked time periodic dynamics (Comb 1, Comb 2, Comb 3 and Comb 4) and complex dynamics.

The experimental results presented in the following demonstrate the existence of unlocked time periodic dynamics beyond the injection locking solution in the plane of injection parameters. The injection strength is calculated by estimating the fiber loss ratio between the modulator and

the input of the injected laser. The power displayed by the modulator is always multiplied by the loss ratio to determine the power received by the injected laser. We define $\kappa = \frac{P_{m}*\gamma}{P_{SL}}$, where γ is the fiber loss ratio, P_m and P_{SL} are the power of the modulator output and injected laser output without injection, respectively. Figure 2 shows the mapping of the qualitatively different dynamics of the injected laser for Ω = 5 GHz. The bias current is fixed at 1.5 times the threshold current, i.e, about 12 mA. Since the frequency comb injection is a modulation of power, injection locking is not a single line optical spectrum but shows three optical lines. The central line has the frequency of the comb line that is the less detuned from the injected laser. The other two lines are strongly supressed, hence leading to the (SA) of the central comb line. The SA regions are found at detuning values close to the frequency positions of the injection comb lines. The SA regions of the side comb lines are found to be smaller than the one of the central comb line as a consequence of the asymmetry of the injected comb. When the injected comb lines have the same amplitude, their corresponding SA regions have comparable sizes [28]. No SA region was observed for the side comb lines when $\kappa > 0.02542$. By contrast the SA region of the central comb line continues until $\kappa = 0.1144$ and bifurcates to a new time-periodic dynamics called "comb 2". The transition between the SA and the "comb 2" region is characterised by an increase of the power in each comb line and the appearance of new comb lines. Around the bifurcation point, the main comb line changes its frequency position, i.e, the comb line that contains the maximum power is not the comb line that shows the smallest detuning from the injected laser frequency anymore. Besides the new comb solution "comb 2" connected to the SA region, another region of frequency comb far from the SA region is created, referred to as "comb 3" in Fig. 2. This new comb region starts to appear when the detuning is close to $\Delta\nu$ = 10 GHz for an injection strength of $\kappa = 0.06355$ and the region expands upon increase of the injection strength towards negative detuning. Other new comb regions called "comb 1" and "comb 4" are observed when the detuning frequency is close to $\Delta\nu = -14$ GHz and $\Delta\nu$ = 14 GHz, respectively. These regions are small such that we were not able to define their size with high precision due to the limits in the fine tuning of the injection parameters. Besides the dynamics of SA and new comb regions, the other dynamics are identified as being complex dynamics including period one, period two, higher others period and quasi-periodicity; example of which will be shown in the following text.

Next, we analyse the impact of the injected comb spacing on the new frequency comb dynamics. The map in Fig 2 corresponds to the case when the injected comb spacing Ω = 5 GHz is close to the relaxation oscillation frequency of the injected laser (4.8 GHz). Figure 3 shows the dynamical mapping for Ω = 2 GHz. We observe three regions of new comb solution stated as "comb 1", "comb 2", and "comb 3". We identify the other dynamics as being complex dynamics. Unlike the case for Ω = 5 GHz , not only is the SA region of the central comb line connected to a new frequency comb region, but also the SA region of the side comb line at -2 GHz. Despite the fact that the locking region of the comb line at -2 GHz is connected to the "comb2" region, its locking area remains very narrow. It is worth mentioning that besides these regions of comb solutions, very narrow and isolated regions of combs are found inside the regions of complex dynamics but these comb solutions are weakly stable and easily destabilize to more irregular pulsing dynamics. The new comb regions appear always when the detuning frequency is close to a multiple of the injected comb spacing and they extend with the injection strength. In agreement with the map in Fig 2, the dynamics of these new comb solutions differ from one region to another.

Figure 4 shows the optical spectra and corresponding time series for the case of Ω = 5 GHz. The positions of these optical spectra are identified in the mapping of Fig. 2 by the letters a, b, c, and d. The detuning is fixed to $\Delta\nu = -0.5$ GHz and Ω = 5 GHz. The red arrow in each optical spectra indicates the position of the central line of the injection comb. When varying the injection strength, the injected laser output shows in Fig. 4 (a) injection locking SA of the central injected comb line with a side comb line suppression ratio of 20 dB. Figure 4 (b) corresponds to

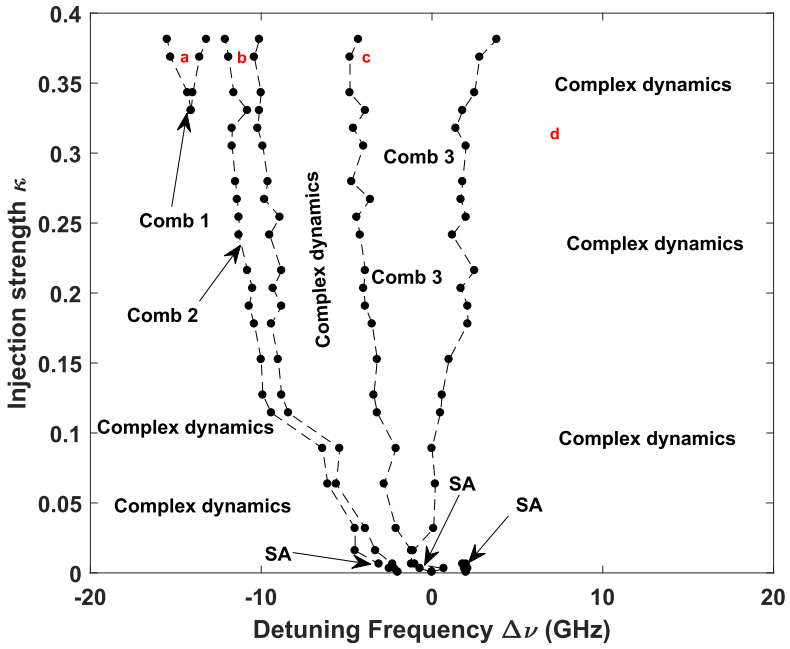

Fig. 3. Nonlinear dynamics mapping of single frequency laser subject to a frequency comb injection for $\Omega = 2$ GHz. We observe Several regions: SA, Unlocked time periodic dynamics (Comb 1, Comb 2 and Comb 3) and complex dynamics.

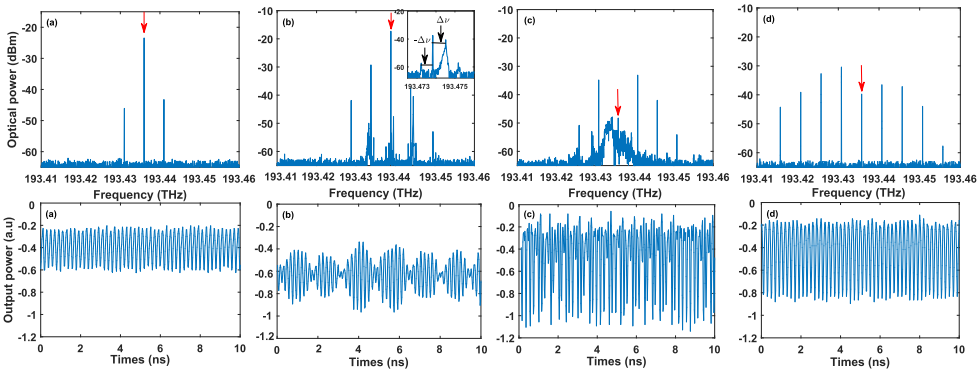

Fig. 4. Optical spectra and corresponding times series when varying the injection strength κ for fixed comb spacing $\Omega = 5$ GHz and detuning $\Delta\nu = -0.5$ GHz. The injected laser output shows the following dynamics: (a) Injection locking at $\kappa = 0.0045$, (b) Wave mixing at $\kappa = 0.025$, (c) complex dynamics at $\kappa = 0.061$ and (d) frequency comb at $\kappa = 0.15$. The red arrow in each optical spectra indicated the position of the central injected comb line.

a modulation as a result of nonlinear wave mixing. When the detuning is close to the limit of the SA region, the injected laser output is always a nonlinear wave mixing between the comb spacing and detuning. When the detuning is equal to a fraction of the comb spacing, this wave mixing leads to harmonic locking as observed in [17, 22]. The dynamics bifurcates to a more complex dynamics as shown in Fig. 4 (c). The detailed chaotic properties shall be discussed elsewhere.

Fig. 4 (d) then corresponds to an unlocked time-periodic dynamics which is a new frequency comb as discussed earlier. Upon increasing the injection strength steadily within the "comb 2" region, the laser leaves the injection locking to a comb which is characterized by the appearance of new comb lines and by a frequency offset of the main comb line with respect to the injected comb line, and by different amplitudes for each comb line.

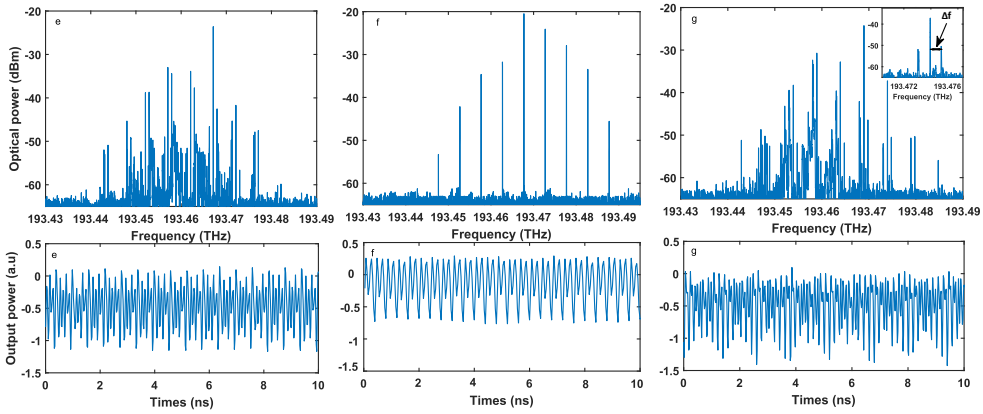

Fig. 5. Optical spectra and corresponding times series when varying the detuning $\Delta\nu$ for fixed comb spacing $\Omega = 5$ GHz and injection strength $\kappa = 0.36$ GHz. We observe: (e) and (g) Wave mixing at $\Delta\nu = 5.4$ GHz and $\Delta\nu = 9.1$ GHz, respectively, (f) new frequency comb at $\Delta\nu = 8$ GHz. The letters (e), (f) and (g) are indicated on the map of Fig. 2

Further insight into the stability of the new comb solutions is given in Fig. 5, where the optical spectra are shown for a fixed $\kappa = 0.36$ and detuning $\Delta\nu$ being swept across the comb3 region. When the detuning is sufficiently close to the value that leads to the observation of the new comb region, a dynamic of wave mixing take places with additional peaks in between the comb lines being separated by Δf as can be seen in Fig. 5 (e) and (g). When varying the detuning from negative to positive values, these additional peaks progressively disappear as the detuning gets close to zero, leading to a stable frequency comb solution as shown in Fig. 5 (f) .

Figure 6 shows the optical spectra and corresponding time series for the case of $\Omega = 2$ GHz. The positions of these optical spectra are identified in the mapping of Fig. 3 by the letters a, b, c, and d. The red arrow indicates the position of the central line of the injected comb and the black arrow indicates the injected laser free-running frequency. Figures 6 (a)-(c) correspond to new frequency combs in the regions "comb 1", "comb 2", and "comb 3", respectively. These figures are obtained for fixed injection strength $\kappa = 0.3686$, but different detuning values. The comparison between Fig. 6 (a), (b) and (c) shows that the injection parameters can be used to precisely tune the comb properties, i.e, number of comb lines and power distribution among comb lines. It is also important to highlight that the comb shown in Fig. 6 (a) is a remarkably stable comb dynamics obtained for a detuning of more than 7 times the injection comb spacing. In the single frequency injection, the stable dynamics is a stationary dynamics whose stability is bounded by the locking range [5]. That locking range is typically of maximum few GHz and is enhanced in specific laser systems that incorporate quantum dots [29, 30]. In the comb injection, by contrast, the stable dynamics is a fundamental comb dynamics that repeats the same spacing for the comb lines as the injected comb. As shown here, that dynamics is observed in several regions of the injection parameters that by far exceed the range of parameters corresponding to selective amplification of the injected lines.

Figure 7 shows the analysis of the new frequency comb properties. Figure 7 (a_1) shows the

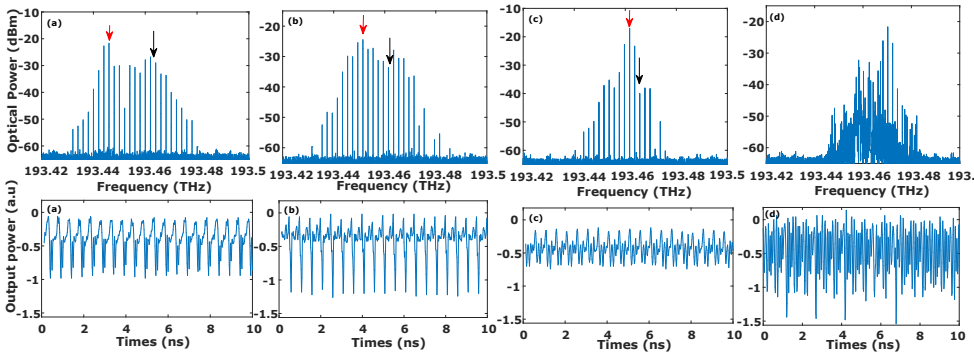

Fig. 6. Optical spectra and corresponding times series for fixed comb spacing to $\Omega = 2$ GHz: (a) Unlocked time periodic dynamics in "comb 1" region at $\kappa = 0.3686$ and $\Delta\nu = -15$ GHz, (b) Unlocked time periodic dynamics in "comb 2" region at $\kappa = 0.3686$ and $\Delta\nu = -10.2$ GHz, (c) Unlocked time periodic dynamics in "comb 3" region at $\kappa = 0.3686$ and $\Delta\nu = -3.8$ GHz and (d) complex dynamics at $\kappa = 0.3177$ and $\Delta\nu = 5.7$ GHz.

optical spectrum from which we measure the spectral width at half-maximum. The pulse width in the corresponding time-series is shown in Fig. 7 (a_2). Figure 7 (b) plots the time-bandwidth product,i.e, product between the pulse width at half-maximum and the spectral width at half-maximum. We observe that the time-bandwidth product increases with the injection strength from 0.93 at $\kappa = 0.1398$ and $\Delta\nu = -3$ GHz and reaches at most the value 1.14 at $\kappa = 0.3635$ and $\Delta\nu = -3$ GHz which is close to 3 times the Fourier limit ~ 0.44 for a Gaussian pulse shape. This indicates that the pulse width is not only determined by the increase of spectral bandwidth, but also that there is a dependency on the phase of the comb lines. This is in very good agreement with our theoretical findings in [24]. In Fig. 7 (c), for $\Omega = 5$ GHz and $\Delta\nu = -3$ GHz, we show the pulse width and the corresponding number of output comb lines of the injected laser as a function the injection strength (κ) within the parameter range corresponding to the new frequency comb region (comb2) in Fig. 2. The pulse width decreases with the injection strength while the corresponding number of output comb lines in the injected laser increases which is in excellent agreement with our previous theoretical prediction in [24]. We also checked that the number of output comb lines increases when increasing the bias current of the injected laser. To evaluate the performance of each new frequency comb region, we calculate the number of comb lines in regions labelled comb1, comb2, comb3 of Fig. 3. In Fig. 7 (d), we plot the number of comb lines in the injected laser output for fixed κ when varying $\Delta\nu$. The number of output comb lines is large in the new frequency comb region far from the SA region and decreases to reach a minimum in the region of new comb which is connected to the SA region of the central comb line. In the "comb3" region, for fixed κ, when we change the detuning from negative to positive values, we observe an abrupt increase of the number of lines in the optical spectrum. This result confirms our numerical analysis in [24]. The injection experiment therefore provides a very fine tuning of the comb properties in the injected laser.

3. Numerical simulations

As already introduced in Ref. [4], the laser system can be modelled by the following rate equations. The electrical field $E(t)$ in the injected laser under frequency comb injection is written as [4]:

$$\frac{dE(t)}{dt} = [i\omega(N) + \frac{1}{2}(G(N) - \frac{1}{\tau_p})]E_S(t) + E_M(t). \quad (1)$$

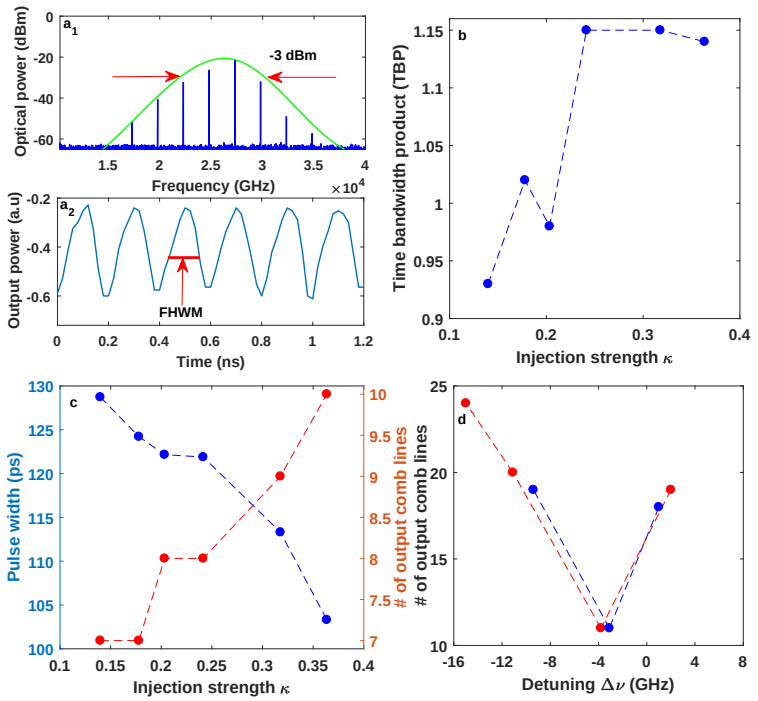

Fig. 7. Control of the output comb properties. (a_1) and (a_2) optical spectrum in comb 2 region in the map of Fig. 2 (a) at $\kappa = 0.1398$ and the corresponding time series of the output power, (b) corresponding time-bandwidth product of the pulse width, (c) pulse width at half maximum on the left vertical axis and the number of output comb line of the injected laser on the right vertical axis for fixed $\Omega = 5$ GHz and detuning $\Delta\nu = -3$ GHz when varying the injection strength, (d) number of output comb lines in different comb regions as a function of detuning frequency $\Delta\nu$ for fixed $\Omega = 2$ GHz.

Here $E_S(t)$ and $E_M(t)$ are respectively the complex fields of the injected laser and the injected comb, i is the imaginary number, N is the carrier density, $\omega(N)$ and G(N) are respectively the angular optical frequency and the differential gain of the injected laser. laser and τ_p is the photon lifetime. The complex electrical field of the injected frequency comb $E_M(t)$ and injected laser $E_S(t)$ can be written as:

$$E_M(t) = \sum_j E_j(t) e^{i(2\pi\nu_j t + \varphi)}, \tag{2}$$

$$E_S(t) = E(t) e^{i(2\pi\nu_0 t + \phi(t))}, \tag{3}$$

Here $E_j(t)$ and $E(t)$ are the amplitudes of the j-th comb-line and of the injected laser. ν_j and ν_0 are the frequencies of the j-th combs-line and of the injected laser. $\Delta\nu_j = \nu_j - \nu_0$ is the detuning between the injected and j-th comb mode. φ and ϕ are respectively the initial phase of each comb-line and the phase of the injected laser. In our study wee set the initial phase of each comb-line to 0. After including the injection field, the amplitude, the phase, and the carrier density rate equations can be rewritten as:

$$\dot{E}(t) = \frac{1}{2} G_N \Delta N(t) E(t) + \sum_j E_j \cos(2\pi\Delta\nu_j t - \phi(t)), \tag{4}$$

$$\dot{\phi}(t) = \frac{1}{2}\alpha G_N \Delta N(t) + \sum_j \frac{E_j}{E(t)} \sin(2\pi\Delta\nu_j t - \phi(t)), \tag{5}$$

$$\dot{N}(t) = R_p - \frac{N(t)}{\tau_s} - G_N \Delta N(t) E(t)^2 - \frac{E(t)^2}{\tau_p}. \tag{6}$$

In these equations, $\Delta N(t) = N(t) - N_{th}$ with N_{th} the threshold carrier density, α is the linewidth enhancement, R_p is the pump rate and τ_s is the carrier lifetime. We write E_{inj} as the total amplitude of the injected field.In the following, we shall use κ for the injection strength with $\kappa = \frac{E_{inj}}{E0}$ where E_0 is the field amplitude of the laser without optical injection. The semiconductor laser parameters are taken as [24] : α=3, $G_N = 7.9 \times 10^{-13}\ m^3 s^{-1}$, $N_{th} = 2.91924 \times 10^{24}\ m^{-3}$, $\tau_s = 2 \times 10^{-9}$ s, $\tau_p = 2 \times 10^{-12}$ s and $R_p = 1.5 R_{th}$ with the pump rate at threshold $R_{th} = 1.8 \times 10^{33}\ m^{-3} s^{-1}$,.

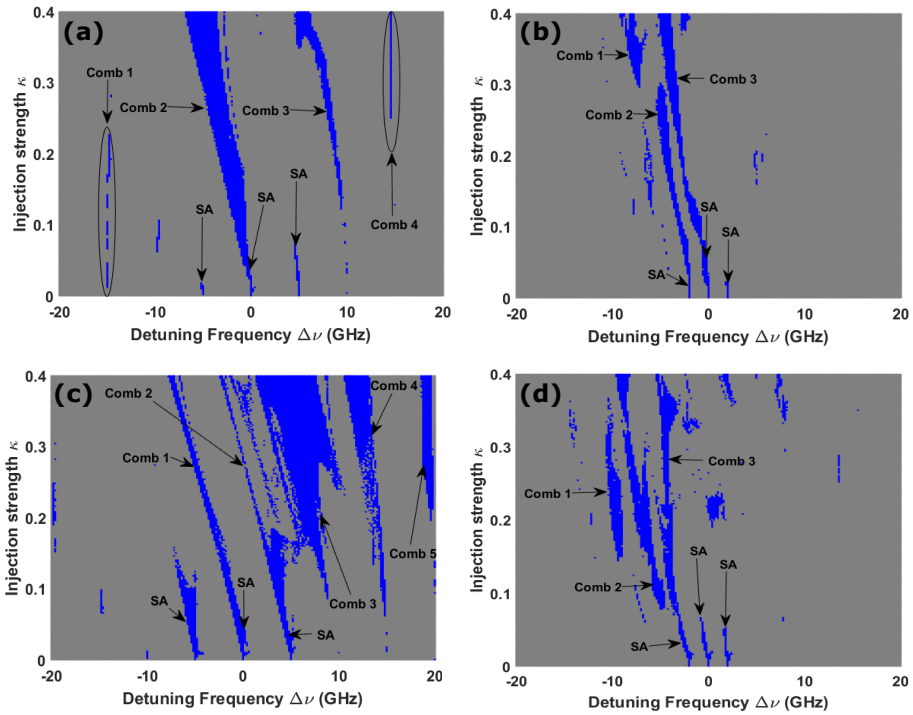

Fig. 8. Numerical mapping of a semiconductor laser subject to optical frequency comb injection. (a) and (b), an asymmetric comb injection similar to the experimental conditions for $\Omega = 5$ GHz and $\Omega = 2$ GHz, respectively. (c) and (d) are the corresponding mappings when all injected comb lines have instead the same amplitude. The blue and gray part correspond to the time periodic dynamics and unlocked chaotic dynamics, respectively. Different regions observed: SA, Comb 1, comb 2, comb 3, comb 4 and comb 5 unlocked time periodic dynamics.

Figure 8 (a) and (b) show the numerical mapping of a single frequency laser under an asymmetric frequency comb injection in the plane of the injection parameters. These figures should be compared with the Fig. 2 and Fig. 3, respectively. The injected laser is biased at 1.5 times threshold current with an injected comb of three frequency lines. To plot these map we follow the successive maxima of the radio frequency spectra and then calculate the difference between their corresponding frequencies. We consider a dynamics to be a frequency comb when

this difference is always equal to the injected comb line spacing. The injected comb lines do not have the same amplitude, i.e, the injected comb is asymmetric. The central comb line has more power than the side comb lines. In Fig. 8 (a) and (b), to realistically model the experiment, we consider that the difference between the amplitude of the central comb line and the side comb lines is 12 dB. The theoretical mapping reproduces the experimental findings qualitatively and even for some features quantitatively with very good agreement. In these maps, the regions shaded in blue correspond to the time-periodic dynamics, i.e., the SA or the new frequency comb region. The region shaded in grey corresponds to any other dynamics that we previously categorised as complex dynamics. Figure 8 (a) and (b) correspond to the numerical mapping for fixed comb spacing to Ω = 5 GHz and Ω = 2 GHz, respectively. Here, we define SA as the case of an injection locking dynamics for which the ratio between the power of the comb line that shows the smallest detuning from the injected comb and the next strongest comb line is more than 10 dB. Our numerical findings reproduce qualitatively the experimental results in which the asymmetry of the injected comb impacts much on the size of the three SA regions. The smaller is the power of one comb line in the injection comb, the narrower is its SA region. In the map of Fig. 8 (a), we observe four regions of frequency combs called "comb 1", "comb 2" , "comb 3" and "comb 4". The small regions of comb called "comb 1" and "comb 4" in the mapping appear when the detuning is $\Delta\nu = -14.6$ GHz and $\Delta\nu = 14.6$ GHz. This theoretical observation is in very good agreement with the experiment. In Fig. 8 (b), we observe three regions of new frequency combs called "comb 1", "comb 2" and "comb 3". Like for Ω = 5 GHz, the map shows as many SA regions as the number of the injected comb lines and these SA regions are separated in the detuning values by the comb spacing. Furthermore, for the case of Ω = 2 GHz, two SA regions connected to the region of combs and additional comb regions are observed. The comb regions extend when increasing the injection strength, as also found in the experiment. In both cases, i.e, Fig. 8 (a) and Fig. 8 (b), the SA regions corresponding to each of the injection comb lines are not of equal size, which is the result of the asymmetry of the injection comb as will be confirmed afterwards. The smaller is the injected comb spacing, the greater is the effect of the asymmetry of the injected comb on the SA regions. In both cases, the fact that comb 2 and comb 3 regions shift towards negative detuning when the injection strength increases is linked to the linewidth enhancement factor α. Indeed, For $\alpha \to 0$, these regions are more symmetric and would even be tilted towards positive detuning if α would be negative. To better evaluate the impact of the injected comb asymmetry on the laser dynamics, we show in Fig. 8 (c) and (d) the numerical mapping when injecting a symmetrical comb, i.e., the injected comb lines have the same amplitude. All other parameters are kept fixed. Figure 8 (c) and (d) correspond to the numerical mapping for fixed Ω = 5 GHz and Ω = 2 GHz, respectively. In both case, the SA regions of the three injected comb lines have almost the same size. For Ω = 5 GHz, the comb 1 region in Fig. 8 (a) has disappeared and the comb 2 region of Fig. 8 (a) corresponds to the comb 1 region of Fig. 8 (c), but is now much smaller. The SA region of the comb line close to 2 GHz detuning is now connected to a new frequency comb region called "Comb 2" in Fig. 8 (c). When increasing the detuning toward positive value, three large new comb regions called "Comb 3", "Comb 4" and "Comb 5" are observed around 10, 15 and 20 GHz which correspond to the multiples of the injected comb spacing. It is important to note that the "Comb 3" and "Comb 4" regions are observed in the same injection parameter plane as their homonyms in Fig. 8 (a). When the comb spacing is Ω = 2 GHz, Fig. 8 (d), only the SA region of the comb at -2 GHz is connected to a new comb solution called "Comb 3" in the mapping. It should be noted that a new comb solution called "Comb 2" appears when the detuning is close to -4 GHz which is a multiple of the injected comb spacing. This new comb solution becomes larger with the injection strength and it is rich in number of lines and much wider than the "comb 3". For large detuning value, close to -8 GHz which corresponds to 4 times the injected comb spacing, we observe another new comb region called "comb 1". The dynamics of the comb solutions differ from a region of

comb to another.

4. Conclusion

In conclusion, we have demonstrated experimentally and numerically the nonlinear dynamics of frequency combs with optical injection. By varying either the injection parameters (injection strength, detuning) or the comb properties (number of line, comb spacing) we identify a rich variety of nonlinear dynamics including: SA of comb line, wave mixing between comb lines and frequencies at detuning values, comb dynamics and irregular chaotic pulsing. Most importantly, the comb dynamics are observed even for very large detuning values, being several times the injection comb spacing. The comb properties including number of comb lines and relative amplitudes of comb lines can be tuned to a large extend by the injection parameters. Finally the experiment reveals the importance of the asymmetry of the injected comb in the observed dynamics. This experiment and the excellent agreement with numerical simulations motivate further analysis of more complex features such as injection of a very larger number of comb lines and injection into a multimode laser.

Finding: The presented study is funded by the Chaire Photonique: Ministère de l'Enseignement Supérieur, de la Recherche et de l'Innovation; Région Grand-Est; Département Moselle; European Regional Development Fund (ERDF); Airbus GDI Simulation; CentraleSupélec; Fondation CentraleSupélec. Fondation Supélec and Metz Metropole. Fonds Wetenschappelijk Onderzoek (FWO) Vlaanderen Project No.G0E5819N.

Disclosures The authors declare no conflicts of interest.

References

1. T. Simpson, J. Liu, and A. Gavrielides, "Bandwidth enhancement and broadband noise reduction in injection-locked semiconductor lasers," IEEE Photonics Technol. Lett. **7**, 709–711 (1995).
2. T. Erneux, *Applied delay differential equations*, vol. 3 (Springer Science & Business Media, 2009).
3. K. Panajotov, M. Sciamanna, H. Thienpont, and A. Uchida, "Impact of light polarization on chaos synchronization of mutually coupled vcsels," Opt. letters **33**, 3031–3033 (2008).
4. F. Mogensen, H. Olesen, and G. Jacobsen, "Locking conditions and stability properties for a semiconductor laser with external light injection," IEEE J. Quantum Electron. **21**, 784–793 (1985).
5. S. Wieczorek, B. Krauskopf, T. B. Simpson, and D. Lenstra, "The dynamical complexity of optically injected semiconductor lasers," Phys. Reports **416**, 1–128 (2005).
6. M. Sciamanna and K. A. Shore, "Physics and applications of laser diode chaos," Nat. photonics **9**, 151–162 (2015).
7. K. Otsuka and H. Kawaguchi, "Period-doubling bifurcations in detuned lasers with injected signals," Phys. Rev. A **29**, 2953 (1984).
8. T. Mukai and K. Otsuka, "New route to optical chaos: Successive-subharmonic-oscil-lation cascade in a semiconductor laser coupled to an external cavity," Phys. review letters **55**, 1711 (1985).
9. V. Kovanis, A. Gavrielides, T. Simpson, and J.-M. Liu, "Instabilities and chaos in optically injected semiconductor lasers," Appl. physics letters **67**, 2780–2782 (1995).
10. C. Bonatto, M. Feyereisen, S. Barland, M. Giudici, C. Masoller, J. R. R. Leite, and J. R. Tredicce, "Deterministic optical rogue waves," Phys. review letters **107**, 053901 (2011).
11. M. Sciamanna and K. Panajotov, "Route to polarization switching induced by optical injection in vertical-cavity surface-emitting lasers," Phys. Rev. A **73**, 023811 (2006).
12. F. Denis-le Coarer, A. Quirce, P. Pérez, A. Valle, L. Pesquera, M. Sciamanna, H. Thienpont, and K. Panajotov, "Injection locking and polarization switching bistability in a 1550 nm vcsel subject to parallel optical injection," IEEE J. Sel. Top. Quantum Electron. **23**, 1–10 (2017).
13. E. K. Lau, L. J. Wong, and M. C. Wu, "Enhanced modulation characteristics of optical injection-locked lasers: A tutorial," IEEE journal selected topics quantum electronics **15**, 618–633 (2009).
14. P. Bouyer, T. Gustavson, K. Haritos, and M. Kasevich, "Microwave signal generation with optical injection locking," Opt. letters **21**, 1502–1504 (1996).
15. Y.-S. Juan and F.-Y. Lin, "Microwave-frequency-comb generation utilizing a semiconductor laser subject to optical pulse injection from an optoelectronic feedback laser," Opt. letters **34**, 1636–1638 (2009).
16. D. S. Wu, D. J. Richardson, and R. Slavík, "Selective amplification of frequency comb modes via optical injection locking of a semiconductor laser: influence of adjacent unlocked comb modes," in *Integrated Optics: Physics and Simulations,* vol. 8781 (International Society for Optics and Photonics, 2013), p. 87810J.

17. A. S. Tistomo and S. Gee, "Laser frequency fixation by multimode optical injection locking," Opt. express **19**, 1081–1090 (2011).
18. Y. Doumbia, T. Malica, D. Wolfersberger, K. Panajotov, and M. Sciamanna, "Frequency comb customization by controlling the optical injection dynamics," in *Semiconductor Lasers and Laser Dynamics IX,* vol. 11356 (International Society for Optics and Photonics, 2020), p. 113560G.
19. S. P. Ó. Duill, P. M. Anandarajah, F. Smyth, and L. P. Barry, "Injection-locking criteria for simultaneously locking single-mode lasers to optical frequency combs from gain-switched lasers," in *Physics and Simulation of Optoelectronic Devices XXV,* vol. 10098 (International Society for Optics and Photonics, 2017), p. 100980H.
20. D. S. Wu, R. Slavík, G. Marra, and D. J. Richardson, "Phase noise and jitter characterization of pulses generated by optical injection locking to an optical frequency comb," in *Frontiers in Optics,* (Optical Society of America, 2012), pp. FW2A–3.
21. A. Gavrielides, "Comb injection and sidebands suppression," IEEE J. Quantum Electron. **50**, 364–371 (2014).
22. K. Shortiss, B. Lingnau, F. Dubois, B. Kelleher, and F. H. Peters, "Harmonic frequency locking and tuning of comb frequency spacing through optical injection," Opt. Express **27**, 36976–36989 (2019).
23. S.-C. Chan and W. K. Tang, "Chaotic dynamics of laser diodes with strongly modulated optical injection," Int. J. Bifurc. Chaos **19**, 3417–3424 (2009).
24. Y. Doumbia, T. Malica, D. Wolfersberger, K. Panajotov, and M. Sciamanna, "Optical injection dynamics of frequency combs," Opt. Lett. **45**, 435–438 (2020).
25. A. C. Bordonalli, M. J. Fice, and A. J. Seeds, "Optical injection locking to optical frequency combs for superchannel coherent detection," Opt. express **23**, 1547–1557 (2015).
26. R. Zhou, T. Shao, M. D. G. Pascual, F. Smyth, and L. P. Barry, "Injection locked wavelength de-multiplexer for optical comb-based nyquist wdm system," IEEE Photonics Technol. Lett. **27**, 2595–2598 (2015).
27. J. Subías, C. Heras, J. Pelayo, and F. Villuendas, "All in fiber optical frequency metrology by selective brillouin amplification of single peak in an optical comb," Opt. express **17**, 6753–6758 (2009).
28. M. S. Pramod, T. Yang, K. Pandey, M. Giudici, and D. Wilkowski, "Selective injection locking of a multi-mode semiconductor laser to a multi-frequency reference beam," The Eur. Phys. J. D **68**, 186 (2014).
29. B. Kelleher, D. Goulding, S. Hegarty, G. Huyet, E. Viktorov, and T. Erneux, "Optically injected single-mode quantum dot lasers," in *Quantum Dot Devices,* (Springer, 2012), pp. 1–22.
30. A. Hurtado, J. Mee, M. Nami, I. D. Henning, M. J. Adams, and L. F. Lester, "Tunable microwave signal generator with an optically-injected 1310nm qd-dfb laser," Opt. express **21**, 10772–10778 (2013).